JOURNAL OF VIROLOGY, June 2011, p. 5708–5717 Vol. 85, No. 12
0022-538X/11/$12.00 doi:10.1128/JVI.02393-10

Oncolytic Vesicular Stomatitis Virus Induces Apoptosis in U87 Glioblastoma Cells by a Type II Death Receptor Mechanism and Induces Cell Death and Tumor Clearance *In Vivo*▽

Zachary D. Cary,[1] Mark C. Willingham,[2] and Douglas S. Lyles[1]*

Department of Biochemistry[1] and Department of Pathology,[2] Wake Forest University School of Medicine, Winston Salem, North Carolina 27157

Received 17 November 2010/Accepted 22 March 2011

Vesicular stomatitis virus (VSV) is a potential oncolytic virus for treating glioblastoma multiforme (GBM), an aggressive brain tumor. Matrix (M) protein mutants of VSV have shown greater selectivity for killing GBM cells versus normal brain cells than VSV with wild-type M protein. The goal of this research was to determine the contribution of death receptor and mitochondrial pathways to apoptosis induced by an M protein mutant (M51R) VSV in U87 human GBM tumor cells. Compared to controls, U87 cells expressing a dominant negative form of Fas (dnFas) or overexpressing Bcl-X_L had reduced caspase-3 activation following infection with M51R VSV, indicating that both the death receptor pathway and mitochondrial pathways are important for M51R VSV-induced apoptosis. Death receptor signaling has been classified as type I or type II, depending on whether signaling is independent (type I) or dependent on the mitochondrial pathway (type II). Bcl-X_L overexpression inhibited caspase activation in response to a Fas-inducing antibody, similar to the inhibition in response to M51R VSV infection, indicating that U87 cells behave as type II cells. Inhibition of apoptosis *in vitro* delayed, but did not prevent, virus-induced cell death. Murine xenografts of U87 cells that overexpress Bcl-X_L regressed with a time course similar to that of control cells following treatment with M51R VSV, and tumors were not detectable at 21 days postinoculation. Immunohistochemical analysis demonstrated similar levels of viral antigen expression but reduced activation of caspase-3 following virus treatment of Bcl-X_L-overexpressing tumors compared to controls. Further, the pathological changes in tumors following treatment with virus were quite different in the presence versus the absence of Bcl-X_L overexpression. These results demonstrate that M51R VSV efficiently induces oncolysis in GBM tumor cells despite deregulation of apoptotic pathways, underscoring its potential use as a treatment for GBM.

Vesicular stomatitis virus (VSV) is a well-studied negative-strand RNA virus that has been identified as a potential oncolytic virus therapy for brain tumors (29, 30, 51, 53). Oncolytic virus therapy is an emerging therapy for cancers that currently lack effective treatment (7, 11). Glioblastoma multiforme (GBM) is a common and highly aggressive brain tumor that has a median survival of approximately 1 year once diagnosed (15). Thus, GBM is a cancer that is widely considered likely to benefit from oncolytic virus therapy. Several clinical trials of oncolytic viruses are ongoing or have already been conducted in patients with GBM (14, 30, 31, 33, 45, 56). To date, at least two VSV oncolytic viruses have been considered by the NIH Recombinant DNA Advisory Committee, a key step toward beginning clinical trials in a variety of cancer types (47, 48).

The selectivity of VSV for cancerous versus normal tissue is due to defects in antiviral responses that cancers develop during tumorigenesis that make them more susceptible to virus infections (4, 5, 42, 43). The selectivity of oncolytic viruses for cancer cells can be enhanced by mutating viral genes involved in suppressing host antiviral responses, which renders these viruses nonpathogenic in normal tissues but effective as oncolytic agents in cancers that have downregulated their antiviral responses. In the case of VSV, the matrix (M) protein is responsible for inhibiting cellular antiviral responses through the general inhibition of host gene expression (2, 9, 10, 13, 43). Mutation of the M protein renders the virus unable to suppress antiviral responses in normal tissues but does not compromise the ability of the virus to replicate in cancers that are defective in their antiviral responses (1, 29, 43). The cancer selectivity of M protein mutant VSV compared to VSV with the wild-type (wt) M protein is illustrated by treatment of human cancer xenografts in immunodeficient mice. Viruses with wt or mutant M protein are similarly effective in reducing tumor burden. However, most immunodeficient mice treated with wt VSV succumb to virus infection, while those treated with M protein mutant virus show no signs of VSV-induced disease (1, 42, 43).

One of the attractive features of VSV as an oncolytic agent is that it is highly cytopathic and induces cell death in nearly all productively infected cells. VSV is a potent inducer of death due to the activation of multiple apoptotic pathways (17, 23). It is important to determine which apoptotic pathways are most crucial for VSV-induced cell killing because many cancers differentially express proteins that regulate apoptosis. Understanding the apoptotic pathways induced by VSV will contribute to understanding the potential outcomes of oncolytic therapy with VSV. The goal of the

* Corresponding author. Mailing address: Department of Biochemistry, Wake Forest University School of Medicine, Medical Center Blvd., Winston Salem, NC 27157. Phone: (336) 716-4237. Fax: (336) 716-7671. E-mail: dlyles@wfubmc.edu.

▽ Published ahead of print on 30 March 2011.

experiments presented here was to determine the apoptotic pathways that are important for the killing of GBM cells by oncolytic M protein mutant VSV.

Previous studies indicated that induction of apoptosis by M protein mutant VSV occurs through different pathways from those used by VSV with wt M protein. The inhibition of host gene expression by wt M protein primarily activates the mitochondrial pathway (6, 17, 22). In contrast, induction of apoptosis by M protein mutant VSV was shown to be mediated by transmembrane death receptors, such as Fas (16). Fas activation induces formation of an intracellular death-inducing signaling complex (DISC) that triggers activation of the initiator caspase-8, ultimately leading to apoptosis via activation of effector caspases such as caspase-3. However, the mitochondrial pathway may also be involved in some cell types (41, 46) since targeting the mitochondrial apoptotic pathway with Bcl-2 inhibitors sensitizes primary chronic lymphocytic leukemia (CLL) cells to an M protein mutant VSV-induced oncolysis (46).

In some cell types, cross talk between the death receptor and mitochondrial apoptotic pathways is required for efficient induction of cell death. Death receptor signaling has been classified as type I or type II, depending on whether signaling is independent of the mitochondrial pathway (type I) or depends on amplification by the mitochondrial pathway (type II) (38, 39). The death receptor pathway can activate the mitochondrial pathway through caspase-8 cleavage of the proapoptotic BH3-only protein Bid. Cleaved Bid (truncated Bid [tBid]) then promotes destabilization of the mitochondria through activation of proapoptotic mitochondrial proteins. Previous results from our laboratory indicated that activation of the mitochondrial pathway by wt VSV is due in part to the activity of Bid (35). This raises the question of whether cross talk through Bid can be an important mechanism of cell death induced by M protein mutant VSV. In results presented here, we show that human GBM cells require a type II death receptor pathway to undergo apoptosis in the presence of an oncolytic M protein mutant VSV, M51R VSV. Unexpectedly, inhibition of apoptosis by overexpression of antiapoptotic Bcl-X_L had little if any effect on the time course of clearance of human GBM xenografts in immunodeficient mice following treatment with M51R VSV. However, the pathological changes in tumors following treatment with virus were quite different in the presence versus the absence of Bcl-X_L overexpression. These results suggest that treatment of GBM tumors with M protein mutant VSV may overcome common mechanisms of cancer resistance to induction of apoptosis.

MATERIALS AND METHODS

Cell lines and virus. U87-MG cells (ATCC HTB-14, referred to here as U87 cells) were cultured in Dulbecco's modified Eagle's medium (DMEM) supplemented with 10% fetal bovine serum. Stable cell lines were generated following the transfection of plasmid DNA using Effectene reagent (Qiagen), according to the manufacturer's protocol. The pcDNA3-Bcl-X_L and control pcDNA3 plasmids have been described previously (35). The pcDNA3.1(+)-puro-dnFas (where dnFas is a dominant negative form of Fas) plasmid was generated similarly to that described in Gaddy and Lyles (16), except that human cDNA was used as a template, and pcDNA3.1(+)-puro was used as the vector. The pIRES2-ZsGreen1-Bcl-X_L (where ZsGreen is *Zoanthus* sp. green fluorescent protein and IRES2 is internal ribosome entry site 2) plasmid was generated by subcloning the Bcl-X_L insert into the pIRES2-ZsGreen1-Lux plasmid. Cells stably transfected with the pcDNA3- or pcDNA3.1(+)-puro-derived plasmid were selected with 800 μg/ml G418 or 0.5 μg/ml puromycin, respectively. Clones were picked using sterile cloning discs. Polyclonal cells stably transfected with pIRES2-ZsGreen1-derived plasmids were sorted via fluorescence-activated cell sorting (FACS), based on the expression of the fluorescent ZsGreen1 protein. M51R VSV was isolated and grown as previously described (24). All cell culture infections were carried out under single-cycle infection conditions at a multiplicity of infection (MOI) of 10 PFU per cell.

Caspase activity assay. Cells were seeded onto six-well plates at 60 to 80% confluence. At various times, cells were infected with M51R VSV or treated with a known inducer of apoptosis. Following infection, floating and attached cells were harvested, and cell lysates were prepared as described previously (50). The fluorogenic substrate DEVD-aminofluorocoumarin (DEVD-AFC; BioMol, Inc.) was added to lysates, and fluorescence was measured over the course of an hour at 37°C using a BMG Labtech POLARstar Omega microplate reader. A protein assay (Bio-Rad) was performed concurrently.

Fas-activating antibody. The Fas-activating antibody, ch.11 (Upstate), was used at a concentration of 1 μg/ml in combination with a low dose of cycloheximide (CHX) (10 μg/ml) as described previously (36).

Immunoblot analysis. Cell lysates were prepared with radioimmunoprecipitation assay (RIPA) buffer containing 1 mM phenylmethylsulfonyl fluoride and 1 mM benzamidine. Lysates were resolved by SDS-PAGE and then transferred to polyvinylidene difluoride (PVDF) using the Invitrogen NuPage system. Membranes were blocked in Tris-buffered saline (TBS; pH 7.5) containing 5% nonfat milk and then probed with antibodies against Bcl-X_L (Cell Signaling Technologies), Bid (Santa Cruz Biotechnology), and actin (Santa Cruz Biotechnology) as previously described (17). Band intensities were quantified by scanning and analysis using Quantity One (Bio-Rad) software.

Fluorescence microscopy. Cells were seeded on BD Falcon 96-well clear-bottom imaging plates. Following infection with virus, cells were labeled with propidium iodide (PI; Invitrogen) and Hoechst 33258 (Invitrogen) and were then imaged using a BD Pathway 855 instrument. Image analysis was performed using ImageJ software and a macro kindly provided by Peter Antinozzi (Department of Biochemistry, Wake Forest University). Briefly, the number of pixels with intensity above the threshold established in mock-infected cells was determined for each wavelength, and the area of positive staining was measured for each well. The ratio of the PI-positive area to Hoechst-positive area was then calculated for each well. This ratio is approximately equal to the fraction of total cells that are PI positive without the complication of observer bias and with the advantage that all of the cells in the well are analyzed, reducing the variability associated with analyzing a limited number of microscopic fields.

Cell viability assay. Cell viability was assessed by MTT [3-(4,5-dimethylthiazol-2-yl)2 2,5-diphenyl tetrazolium bromide] assay, according to the manufacturer's instructions (Roche Molecular Biochemicals). Cell viability was evaluated, and survival was estimated relative to untreated controls as described previously (23, 35).

RNA interference. U87 cells were transiently transfected with 15 nM Bid small interfering RNA (siRNA) or control siRNA-A (Santa Cruz Biotechnology) using Dharmafect 4 (Thermo Fisher, Dharmacon) transfection reagent according to the manufacturer's instructions. Cells were harvested for immunoblot analysis in order to assess the quality of siRNA transfection.

Time-lapse microscopy. Cells were seeded at approximately 60 to 70% confluence on 24-well dishes. Time-lapse microscopy was performed as described previously (35). Infections were allowed to progress through 48 h.

Subcutaneous tumor model. U87 cells transfected with pIRES2-ZsGreen1-Bcl-X_L or pIRES2-ZsGreen1-Lux were harvested from semiconfluent cultures. Cells were resuspended at 2×10^6 cells/0.1 ml of phosphate-buffered saline (PBS), and for each transgenic cell line, cells were subcutaneously injected in the right, hind-flank of 12 female nude (*nu*/*nu*) mice (six mice per treatment group). Animals were monitored for tumor development and weighed daily. Animals with palpable tumors had their tumor volume measured with calipers, and the volume was calculated as follows: volume = $(\text{width})^2 \times \text{length}/2$. After 1 week, palpable tumors developed (50 to 100 mm^3), and each animal was injected intravenously (i.v.) twice, 3 days apart, with either M51R VSV (1×10^7 PFU) or PBS. Mice were sacrificed when the tumor size approached the predetermined upper size limit of 1,000 mm^3 or 3 weeks after injection with M51R VSV or PBS. The mice were sacrificed at this time in order to determine whether there was residual tumor or signs of VSV-induced pathology. The tumor site and selected tissues (brain, spleen, and lungs) were harvested for histological analysis.

Immunohistochemistry. Tumors generated as described above were harvested 2 days after treatment with M51R VSV or PBS and were fixed in 4% paraformaldehyde overnight, embedded in paraffin, and sectioned at 5 μm. Tissue sections were immunostained for VSV glycoprotein as described previously (3). Cleaved caspase-3 staining was done according to the same protocol, using a monoclonal

antibody that was raised to the large fragment of active caspase-3 (catalog item 9664; Cell Signaling Technology).

Statistical analysis. For most experiments, a Holm-Sidak one-way analysis of variance test was used to determine statistical significance ($P < 0.05$). For fluorogenic caspase-3 assays, replicate experiments were assayed with uniform instrument settings. Analysis of variance was used to determine statistical significance for those experiments where control measurements had a standard deviation that was <20% of the mean. For experiments performed at different times, instrument sensitivity was a major source of variability (standard deviation [SD] greater than 30% of the mean). For these experiments, a paired *t* test was used to determine statistical significance of experimental groups compared to control cells ($P < 0.05$). For analysis of tumor size as a function of time in the *in vivo* experiments, a two-way repeated measures analysis of variance was used to test for statistical significance with the Bonferroni procedure for all pairwise multiple comparisons. Statistical analyses were performed using SigmaStat software (Systat Software, Inc.).

RESULTS

The death receptor pathway is important for M51R VSV-induced apoptosis in GBM cells. Previous experiments using mouse L929 cells indicated that the death receptor pathway was the predominant pathway by which infection with M51R VSV induced apoptosis (16). The purpose of the experiments shown in Fig. 1 was to determine if the death receptor pathway is also important for the induction of apoptosis by M51R VSV in human GBM cells. The U87 cell line was chosen for these experiments since it has been widely used in studies of susceptibility of GBM cells to oncolysis by VSV and other viruses (19, 29, 30, 34, 40, 52, 53). U87 GBM cells were stably transfected with either an empty vector (EV) or a vector expressing a dominant negative form of the Fas death receptor (dnFas). Clonal cell lines were established by antibiotic selection, and clones expressing functional dnFas were identified by their resistance to induction of apoptosis by Fas-activating antibody (ch. 11). Transfected or nontransfected cells were infected with M51R VSV for various periods of time, cell extracts were prepared, and caspase-3-like activity was assessed. M51R VSV induced high levels of caspase-3-like activity in nontransfected and empty vector control cells but induced significantly lower levels in the dnFas cells (Fig. 1A). The extent of inhibition by dnFas expression was similar to that observed in control experiments in which U87 EV- and dnFas-expressing cells were treated with an agonistic antibody (ch.11) to the Fas death receptor (Fig. 1B). Thus, expression of dnFas was able to inhibit the apoptotic pathways leading to caspase-3-like activity in U87 cells infected with M51R VSV.

Caspase-8 is one of the principal initiator caspases in the death receptor pathway of apoptosis. To determine if the activity of caspase-8 was involved in the induction of apoptosis in M51R VSV-infected U87 cells, cells were left untreated or treated with a caspase-8-specific inhibitor (zIETD), a pan-caspase inhibitor (zVAD), or vehicle alone (dimethyl sulfoxide [DMSO]). Cells were then infected for various times, and cell extracts were assayed for caspase-3-like activity (Fig. 1C). Caspase-3-like activity was undetectable in both zVAD- and zIETD-treated U87 cells, consistent with the requirement for caspase-8 activity for activation of caspase-3 in U87 cells infected with M51R VSV. Collectively, the data in Fig. 1 are consistent with results of similar experiments in L929 cells indicating that the death receptor pathway is a major pathway leading to caspase-3 activation in U87 cells.

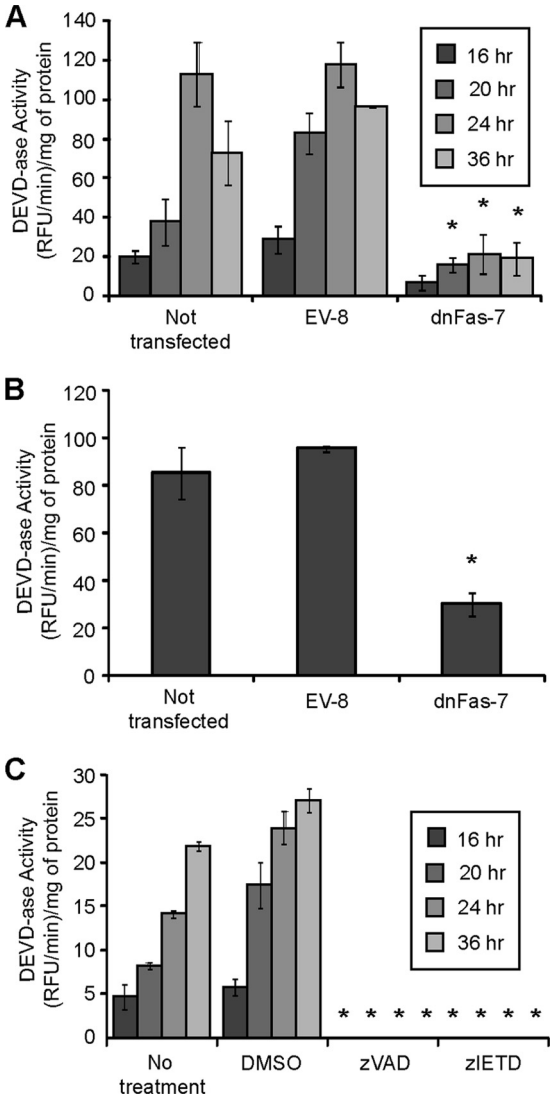

FIG. 1. M51R VSV requires a Fas-mediated pathway to induce apoptosis in GBM cells. (A) U87 cells that were not transfected, empty vector clone 8 (EV-8), and dominant negative Fas clone 7 (dnFas-7) cells were infected with M51R VSV for various periods of time. Cell extracts were prepared, and caspase-3-like activity was assessed. (B) U87, EV-8, and dnFas-7 U87 cells were treated with ch.11 for 12 h and were analyzed as in panel A. (C) Prior to infection, U87 cells were treated for 1 h with DMSO, zVAD, or zIETD. Cells were infected with M51R VSV at various times, and cell extracts were prepared and analyzed as in panels A and B. Asterisks indicate statistical significance ($P < 0.05$) against EV or DMSO control cells at corresponding time points among three independent experiments. Error bars indicate standard errors of the means. RFU, relative fluorescence units.

The mitochondrial pathway is important for apoptosis induced by death receptor and M51R VSV in U87 GBM cells. In addition to the death receptor pathway, the other major apoptotic pathway is the mitochondrial pathway. In order to test the involvement of the mitochondrial pathway, U87 cells were stably transfected with a vector that expressed Bcl-X_L. Clonal populations were selected by antibiotic resistance, and overexpression of Bcl-X_L was tested by immunoblotting. Two clones that had among the highest overexpression of Bcl-X_L were

selected, and their immunoblots are shown in Fig. 2A. Caspase-3-like activity was dramatically reduced in both U87 Bcl-X_L-overexpressing clones infected with M51R VSV (Fig. 2B). These data indicate that the mitochondrial pathway of apoptosis is also required in addition to the death receptor pathway for M51R VSV-induced activation of caspase-3 in GBM cells.

Death receptor signaling has been classified as type I or type II depending on whether signaling is independent of (type I) or depends on (type II) the mitochondrial pathway. The response of U87 cells to infection with M51R VSV resembles a type II response to death receptor ligands. To determine whether the response of U87 cells to Fas receptor ligation is similar to that of type II cells, U87 control and Bcl-X_L-overexpressing clones were treated with ch.11 for 12 h, and caspase-3-like activity was assessed (Fig. 2C). Bcl-X_L overexpression inhibited caspase activation in response to ch.11, similar to the inhibition in response to M51R VSV infection. These data indicate that U87 cells behave as type II cells in response both to Fas receptor ligation and virus infection.

In addition to evaluating caspase activation, the induction of cell death in M51R VSV-infected U87 cells was determined by assessing plasma membrane integrity by propidium iodide (PI) staining. Control or Bcl-X_L-overexpressing cells were mock infected or infected with M51R VSV in the presence or absence of zVAD. At various times postinfection, cells were double labeled with Hoechst and PI (which label the nuclei of all cells and permeable cells, respectively) and analyzed by quantitative fluorescence microscopy. The number of pixels with intensity above the threshold established in mock-infected cells was determined, and the values are expressed as the ratio of the PI-positive area to Hoechst-positive area (Fig. 2D). At early time points postinfection, there was very little PI labeling above the mock-infected controls. However, by 36 h, there was a substantial amount of PI labeling in control cells, which was inhibited by overexpression of Bcl-X_L or treatment with zVAD. These data provide further evidence of a role for the mitochondrial pathway in the induction of cell death in U87 cells by infection with M51R VSV.

Bid is required for M51R VSV-induced apoptosis. Cross talk between pathways during the type II response to death receptor-induced apoptosis is usually mediated by the Bcl-2 family member Bid. Bid is cleaved by caspase-8 to generate the proapoptotic tBid. The cleavage of Bid to tBid was determined through immunoblot analysis by following the disappearance of full-length Bid (Fig. 3A). As a control for normal turnover of Bid, cells were treated with zIETD to inhibit caspase-8 activity or were treated with vehicle (DMSO) alone. Cells were infected for various times with M51R VSV or were treated with ch.11. Immunoblots were quantified by densitometry, and the results of replicate experiments are shown in Fig. 3B. There was a dramatic decrease in the amount of full-length Bid in U87 cells treated with ch.11, which was prevented in the presence of zIETD. The tBid cleavage product produced in cells treated with ch.11 could be detected directly in the same immunoblots upon longer exposure (data not shown). However, in virus-infected cells, the amount of full-length Bid declined over a more prolonged time course, and the tBid cleavage product could not be detected even at prolonged exposures. Thus, if Bid is involved in response to virus infec-

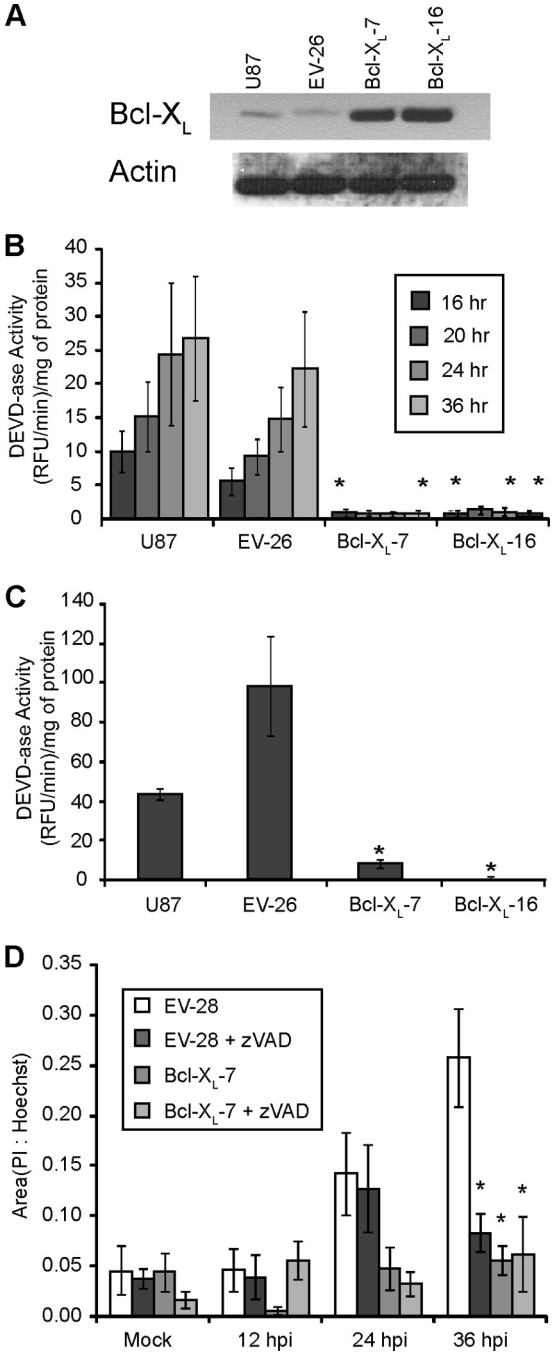

FIG. 2. Bcl-X_L overexpression inhibits caspase-3 activation in M51R VSV-infected GBM cells. (A) U87 cells were stably transfected with a vector that expressed Bcl-X_L or an empty vector control. Clonal populations were selected, and overexpression of Bcl-X_L was tested by immunoblotting. An immunoblot is shown for nontransfected U87 cells, empty vector clone 26 (EV-26), and Bcl-X_L-overexpressing clones 7 and 16 (Bcl-X_L-7 and -16). U87 control and Bcl-X_L-overexpressing clones were infected for various times (B) or treated with ch.11 antibody for 12 h (C), and cell extracts were assessed for caspase-3-like activity. (D) U87 empty vector control and Bcl-X_L-overexpressing clones were infected for various times in the presence or absence of the caspase inhibitor zVAD and stained with Hoechst dye and PI. Cells were then imaged, and the area of Hoechst and PI staining was determined using ImageJ software. Asterisks indicate statistical significance ($P < 0.05$) against EV control cells at corresponding time points among three independent experiments. Error bars indicate standard errors of the means.

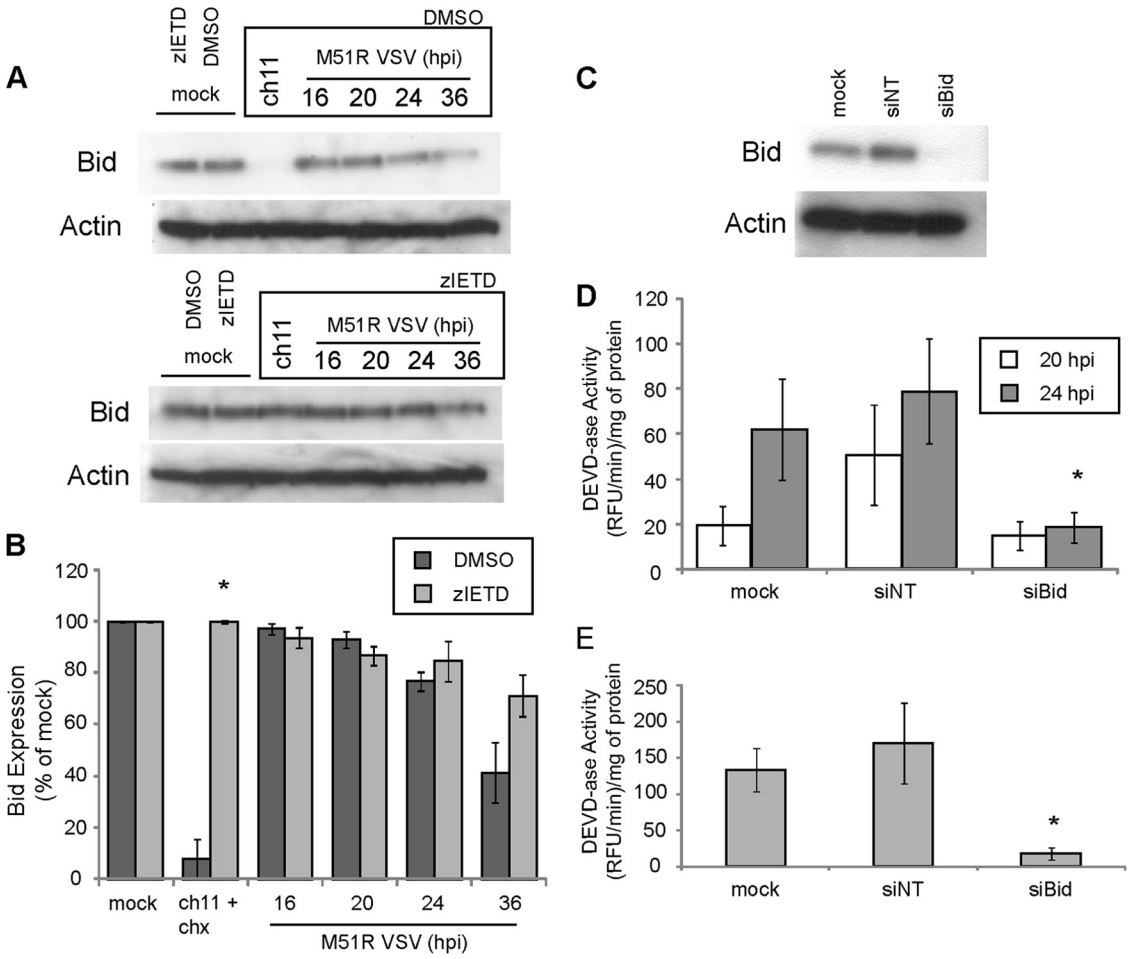

FIG. 3. Bid is required for apoptosis induced during M51R VSV infection in GBM cells. (A) U87 cells were pretreated with DMSO or zIETD prior to treatment with ch.11 (12 h) or at various times of infection with M51R VSV. Cell lysates were prepared, and Bid expression was determined by immunoblotting. (B) Densitometry analysis was preformed on immunoblots similar to those shown in panel A. (C) U87 cells were either mock transfected or transfected with Bid siRNA (siBid) or nontargeting siRNA (siNT), and efficiency of silencing was assessed by immunoblotting. (D) At 48 h posttransfection, cells transfected as in panel C were infected with M51R VSV, and caspase-3-like activity was assessed. (E) Cells transfected as in panel C were treated with ch.11 for 12 h, and caspase-3-like activity was measured. Asterisks indicate statistical significance ($P < 0.05$) against DMSO or nontargeting control cells at corresponding time points among three independent experiments. Error bars indicate standard errors of the means.

tion of U87 cells, it may be due to prolonged generation of small amounts of tBid over the time course of virus infection.

In order to determine if Bid was required for activation of caspase-3 by M51R VSV infection, the expression of Bid was silenced using siRNA. U87 cells were transfected with a nontargeting siRNA or with an siRNA targeting Bid for 48 h (Fig. 3C). Cells were then infected with M51R VSV for 20 and 24 h or treated with ch.11 for 12 h, and caspase-3-like activity was assessed (Fig. 3D and E). Silencing Bid expression significantly reduced caspase-3 activation in cells infected with M51R VSV. Cells silenced for Bid expression and treated with ch.11 antibody also had reduced caspase activity compared to cells that were not transfected or transfected with nontargeting siRNA (Fig. 3E). These results provide further evidence that establish U87 cells as type II cells.

Inhibition of apoptosis does not protect U87 cells from cytopathic effects of M51R VSV infection. Previous analysis of mouse L929 cells indicated that inhibition of apoptosis was sufficient to protect M51R VSV-infected cells from cytopathic effects and cell death (16). However, inhibition of apoptosis in U87 cells by treatment with zVAD or overexpression of Bcl-X_L failed to inhibit M51R VSV-induced cytopathic effects. Control or Bcl-X_L-overexpressing cells were infected with M51R VSV in the presence or absence of zVAD, and the time course of induction of cytopathic effects was determined by time-lapse phase-contrast microscopy. Figure 4 shows examples of the same fields at 0 and 48 h postinfection. By 48 h, control cells had undergone the morphological changes that are characteristic of apoptosis, including cell rounding, membrane blebbing, cell shrinkage, and loss of refractility. Cells treated with zVAD or overexpressing Bcl-X_L underwent cell rounding but did not undergo cell shrinkage and retained their refractility. At this time point, rounded cells may not be dead. These data are consistent with the inhibition of some of the morphological changes associated with apoptosis, but treatment with zVAD, overexpression of Bcl-X_L, or the

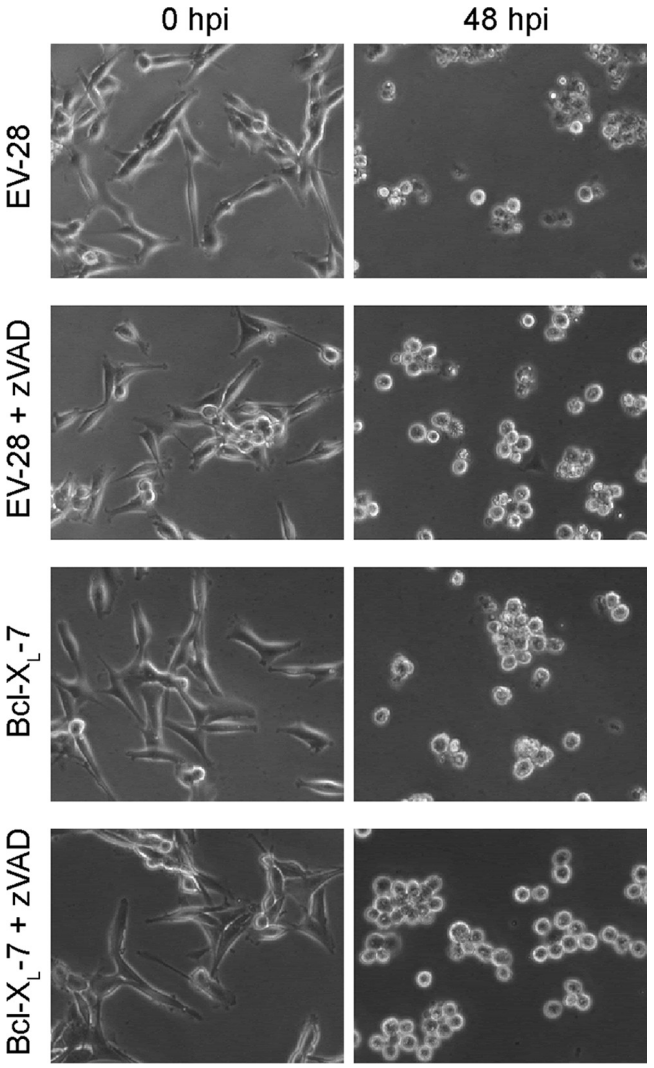

FIG. 4. Cytopathic effects during M51R VSV infection of U87 cells treated with zVAD and overexpressing Bcl-X_L. EV and Bcl-X_L-overexpressing clones were left untreated or were pretreated with zVAD and infected with M51R VSV. Cells were imaged by time-lapse phase-contrast microscopy for at least 48 h. The zero time point and 48-h time point from the same fields are displayed.

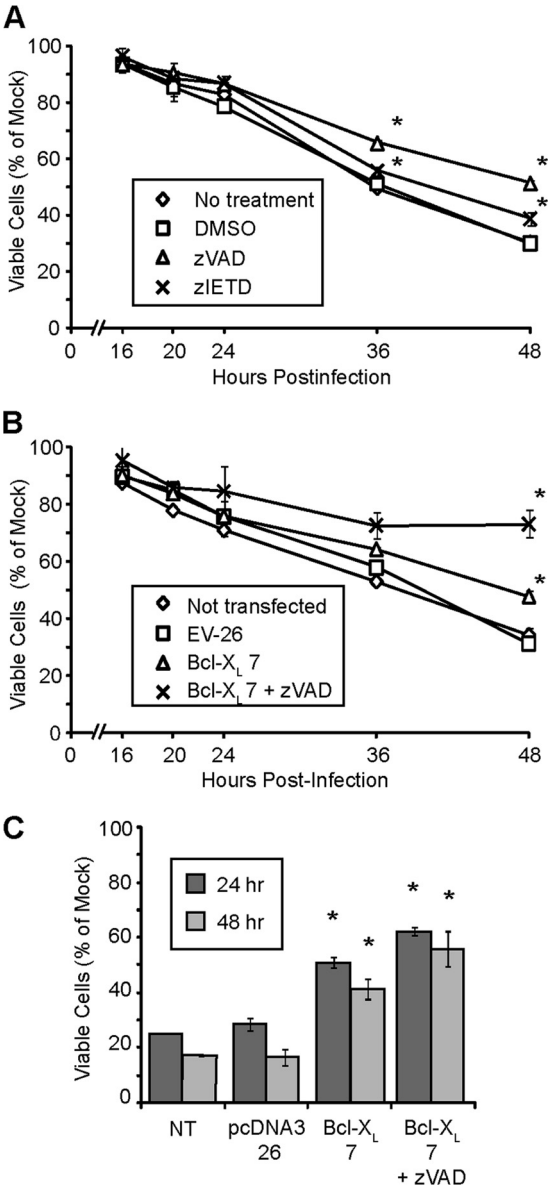

FIG. 5. Loss of viability of U87 cells following M51R VSV infection in the presence of inhibitors of apoptosis. U87 cells that were not treated or pretreated with DMSO, zVAD, or zIETD (A) or empty vector (EV) and Bcl-X_L-overexpressing cells (B) were infected with M51R VSV, and cell viability was determined via an MTT assay. (C) EV and Bcl-X_L-overexpressing clones were treated with ch.11 antibody for 24 and 48 h, and cell viability was determined via MTT assay. A single asterisks indicates statistical significance ($P < 0.05$) against DMSO or nontransfected control cells at corresponding time points; double asterisks indicate statistical significance against Bcl-X_L cells not treated with zVAD. Data are from three independent experiments. Error bars indicate standard errors of the means.

combination of the two was not able to inhibit the induction of cytopathic effects by M51R VSV.

The effect of inhibiting apoptosis in U87 cells upon cell viability was assessed by an MTT assay, which uses ongoing mitochondrial metabolism as a measure of cell viability. Treatment of U87 cells with zVAD or zIETD had only a small effect on the time course of loss of viability following M51R VSV infection (Fig. 5A). Similarly, overexpression of Bcl-X_L had only a small effect on loss of cell viability (Fig. 5B) although the differences from results with control cells were statistically significant at later times postinfection for both caspase inhibitors and Bcl-X_L overexpression. The combination of treatment with zVAD and Bcl-X_L overexpression substantially delayed the loss of viability (Fig. 5B). However, at much later times postinfection, it was apparent that cell death was not prevented but merely delayed (not shown).

Inhibition of apoptosis by Bcl-X_L overexpression and treatment with zVAD also did not fully protect cells from the effects of treatment with Fas-activating antibody ch.11 (Fig. 5C). Treatment of nontransfected or vector control U87 cells with ch.11 reduced cell viability to approximately 15% of control by 48 h posttreatment. Treatment of Bcl-X_L cells with ch.11 in the presence or absence of zVAD resulted in less loss of viability

(40 to 60% of control at 48 h). Similar to results with virus infection, the cells were not fully protected from the induction of cell death.

Overexpression of Bcl-X_L does not delay viral oncolysis *in vivo*. The data presented thus far show that M51R VSV induces a pathway of caspase activation that can be inhibited by the overexpression of Bcl-X_L. This overexpression significantly delays cell death *in vitro*, but in terms of M51R VSV's potential as an oncolytic agent against GBM tumors, it was important to assess if there is an effect of Bcl-X_L overexpression in GBM tumors *in vivo*. Polyclonal populations of transfected U87 cells were used to establish tumors *in vivo* because we found that clonal populations of empty vector control U87 cells formed tumors very inefficiently (unpublished results). Polyclonal cells were produced by transfection with a bi-cistronic vector that expresses either firefly luciferase (ZsG LUX) or Bcl-X_L (ZsG Bcl-X_L) under the control of the cytomegalovirus (CMV) promoter and expresses the *Zoanthus* sp. green fluorescent protein (ZsGreen) under the control of a downstream IRES sequence. ZsGreen-expressing cells were isolated by fluorescence-activated cell sorting. Overexpression of Bcl-X_L in these cells was similar to that of the clonal cell lines analyzed earlier (Fig. 6A). Immunoblot analysis confirmed that the overexpression of Bcl-X_L in the starting cell cultures was maintained in the resulting tumors *in vivo* (Fig. 6A).

Transfected cells were injected subcutaneously into the hind flanks of female nude mice. After 1 week, palpable tumors developed (50 to 100 mm^3); the animals were randomized into treatment and control groups, and each animal was injected intravenously twice, 3 days apart, with either M51R VSV (treatment group) or PBS (control group). Tumor size and mouse weight were then determined daily (Fig. 6B). Control ZsG LUX and ZsG Bcl-X_L tumors grew to the upper size limit in approximately 1 week after inoculation. Mice that received M51R VSV had markedly reduced tumors, and within 21 days after initial inoculation, mice had no tumor present that was detectable during necropsy. Mice did not have any apparent symptoms of VSV infection and did not experience significant weight loss after inoculation with virus similar to previous results (1). Interestingly, the time course of tumor regression was similar for control and Bcl-X_L-overexpressing tumors. This result suggests that Bcl-X_L overexpression has little if any effect on oncolytic tumor clearance in U87 GBM tumors.

Viral antigen expression and caspase-3 activation in tumors were analyzed by immunohistochemistry using antibodies specific for the VSV envelope glycoprotein (G protein [VSV-G]) and cleaved caspase-3, respectively. Tissue sections were obtained 24 h after the second inoculation from animals bearing ZsG LUX and ZsG Bcl-X_L tumors. Tumors taken from animals treated with M51R VSV had focal areas with positive staining for VSV-G (Fig. 7A). There was no obvious difference between tumors derived from ZsG LUX and ZsG Bcl-X_L cells in either the extent or intensity of viral antigen staining. Interestingly, the foci of viral antigen staining were associated with different cytopathic effects depending on whether the tumors were derived from U87 ZsG LUX or ZsG Bcl-X_L cells. VSV-G staining in control ZsG LUX tumors was coincident with areas containing condensed nuclei and nuclear fragments, indicative of apoptotic cell death. This contrasts with the cytopathic effects observed in the ZsG Bcl-X_L tumors, in which few apoptotic bodies could be seen in VSV-G-positive areas. Instead, foci of VSV-G-positive staining were associated with large syncytia (Fig. 7, arrows). Infiltrating inflammatory cells could also be observed in both tumor types but was more obvious in ZsG Bcl-X_L tumors (Fig. 7, arrowheads) without the background of apoptotic cells. When stained for cleaved caspase-3, labeling was more prevalent in infected ZsG LUX tumors than in ZsG X_L tumors (Fig. 7B). The small but detectable amount of cleaved caspase-3 in the ZsG Bcl-X_L tumors was found only in syncytia. This low level of staining is consistent with residual caspase-3 activity observed in infected Bcl-X_L-overexpressing U87 cells *in vitro*. In mock-infected tumors, cleaved caspase-3 could be detected in very few individual cells. These *in vivo* results are consistent with the conclusion that apoptosis induced by M51R VSV is inhibited when Bcl-X_L is overexpressed in GBM cells.

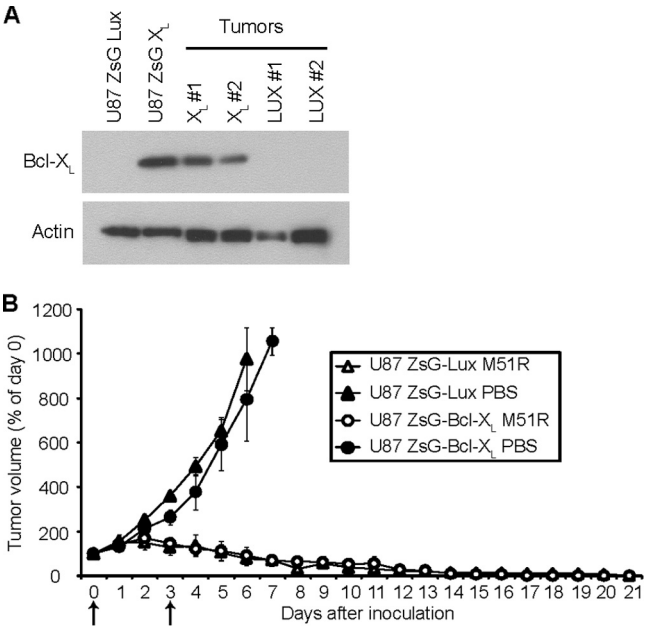

FIG. 6. Bcl-X_L overexpression does not delay tumor clearance *in vivo*. U87 cells transfected with a plasmid expressing Bcl-X_L (U87 ZsG XL) or luciferase (U87 ZsG Lux) were injected subcutaneously into the hind flanks of female nude (*nu*/*nu*) mice. Palpable tumors were allowed to develop for 7 days, and mice were then inoculated intravenously with either M51R VSV or PBS. Mice were inoculated again 3 days later. (A)Tumors from the PBS treatment group were harvested 7 days after the initial inoculation, by which time the tumors had reached the predetermined maximum size limit. The levels of expression of Bcl-X_L were determined by immunoblotting. Shown are data comparing the original cell lines with two tumors derived from each. (B)Tumor size was determined daily. Arrows indicate days of inoculation. All PBS-treated animals developed tumors that grew to the upper size limit and were subsequently sacrificed. Treatment with M51R VSV reduced both luciferase- and Bcl-X_L-expressing tumors to undetectable levels. There was no significant difference between luciferase- and Bcl-X_L-expressing tumors in either the M51R VSV or PBS treatment groups as determined by repeated-measures analysis of variance. The differences between the M51R VSV and PBS treatment groups were statistically significant ($P < 0.05$) beginning on day 4 for luciferase-expressing tumors and on day 5 for Bcl-X_L-expressing tumors. Error bars indicate standard errors of the means.

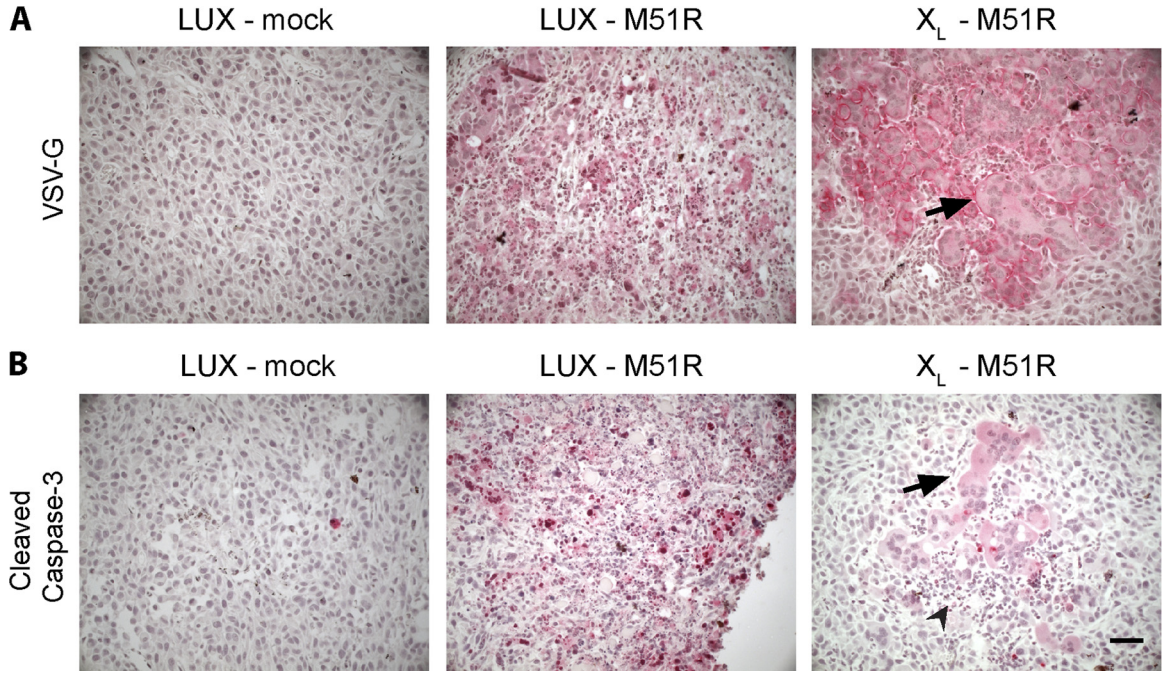

FIG. 7. Expression of viral antigen and cleaved caspase-3 in control and Bcl-X_L-overexpressing tumors infected with M51R VSV *in vivo*. (A) Representative micrographs of tumor sections immunostained for VSV glycoprotein (VSV-G). Red indicates positive immunoreactivity. Large syncytia were seen in infected Bcl-X_L tumor cells (black arrow). (B) Tumor sections were stained for cleaved caspase-3. Low to moderate staining in Bcl-X_L tumor cells was only seen where syncytia had formed (black arrow). Immune infiltrating cells could be clearly identified at the site of syncytium formation (arrowhead). Bar, 30 μm.

DISCUSSION

Much of the attractiveness of VSV as an oncolytic agent is the potency with which it induces apoptosis in infected cells. However, the pathways leading to the biochemical features of apoptosis, such as caspase activation, appear to vary among different cell types. Previous experiments in other cell types have implicated either the death receptor or mitochondrial pathways as the major mechanisms of cell death in response to M protein mutant VSV (16, 17, 23, 41, 46). The data presented here indicate that M51R VSV induces apoptosis via both the death receptor and mitochondrial pathways in U87 GBM cells. The evidence for involvement of the death receptor pathway includes experiments showing that dnFas and chemical caspase-8 inhibition delay activation of apoptosis in response to M51R VSV infection in U87 cells (Fig. 1). However, Bcl-X_L overexpression in U87 cells inhibited caspase-3 activation in the presence of M51R VSV infection as well (Fig. 2). This contrasts with previous results from our laboratory, which determined the pathways activated by M51R VSV in mouse L929 cells (16, 17). In L929 cells, the mitochondrial pathway was activated by M51R VSV infection; however, inhibiting the mitochondrial pathway had no effect on the induction of apoptosis.

The difference in the relative importance of the mitochondrial pathway in L929 versus U87 cells can be readily explained by analogy to the type I versus type II response to death receptor ligands. Collectively, our results indicate that L929 cells respond to M51R VSV infection in the manner of type I cells and that U87 cells respond in the manner of type II cells. The type II cell death response is thought to occur in cells where death-induced signaling complex (DISC) signaling is impaired, either due to poor formation of the DISC itself (38, 39) or because of upregulated inhibitors of the downstream caspase cascade (20, 49). These type II cells thus require an amplification of the death stimulus through the mitochondrial pathway (20, 38, 39, 49). The communication between these two pathways is known to occur through Bid (54, 55). Consistent with this mechanism, silencing Bid expression with siRNA in U87 cells inhibited induction of apoptosis in the presence of M51R VSV (Fig. 3).

Inhibitors of apoptosis (treatment with zVAD and overexpression of Bcl-X_L) do not completely block induction of cytopathic effects in M51R VSV-infected U87 cells (Fig. 4). There are two possible explanations for this result: either there is incomplete inhibition of apoptosis with these inhibitors, or alternative pathways are being activated during infection. It has been shown that VSV induces autophagy in infected cells (27, 28), and we have observed autophagy induction by LC3 I to II cleavage during infection in U87 cells via immunoblotting (data not shown). However, autophagy as a cell death mechanism remains unclear (26). We have also performed experiments to inhibit programmed necrosis, or necroptosis, an alternative form of cell death known to be activated during inhibition of death receptor-induced apoptosis (18). Treatment of U87 cells with necrostatin-1 (an inhibitor of necroptosis) and zVAD did not protect cells from cytopathic effects and cell death (data not shown). There are other potential mechanisms of cell death that may be initiated by the presence of a VSV infection and are potentially important; however, the evidence presented here indicates that even in the presence of

apoptotic inhibitors, U87 cells infected with M51R VSV eventually die. This result also contrasts with results obtained in L929 cells infected with M51R VSV, in which inhibition of induction of apoptosis allows the cells to survive the infection and eventually to clear the virus infection (Daniel F. Gaddy and Douglas S. Lyles, unpublished results). This raises the possibility that inhibition of apoptosis in type I cells allows the cells to survive while inhibition in type II cells does not, perhaps due to extensive damage to mitochondria through the type II mechanism.

Many cancers, including GBM tumors, have deregulated mitochondrial apoptosis pathways, often overexpressing antiapoptotic proteins such as Bcl-X_L (25, 44). This has been a challenge when GBM tumors are treated with chemotherapy since overexpression of Bcl-X_L or other inhibitors of apoptosis usually leads to inhibition of tumor regression in response to treatment. However, we observed efficient tumor regression following treatment with M51R VSV of nude mice bearing U87 tumors that overexpress Bcl-X_L (Fig. 6A). This unexpected result of tumor clearance is likely due to the fact that overexpression of Bcl-X_L delays, but does not prevent, cell death in response to virus infection. The time course of tumor regression, which occurs over 2 to 3 weeks (Fig. 6B), may be too long for the rate at which individual cells die to be a significant factor in this system. This result bodes well for the potential of M51R VSV as an oncolytic agent in that, even in the presence of Bcl-X_L overexpression, oncolytic VSV can reduce tumor burden. However, in a model of CLL, treatment with a small-molecule inhibitor of Bcl-2 accelerated the induction of cell death and accelerated tumor clearance in response to oncolytic VSV (46). Thus, in some tumor systems, the rate at which individual cells die in response to virus infection can be a factor in the rate of tumor regression.

Interestingly, tumors derived from U87 cells that overexpress Bcl-X_L do not appear to have the same pathological changes as control cells when infected *in vivo*. Instead, Bcl-X_L-overexpressing cells form large syncytia *in vivo* (Fig. 7). VSV-infected cells do not normally form syncytia in most cell types; however, mutant viruses have been developed in order to harness this property from other viruses for increased VSV oncolytic potency (12). Ebert et al. found that a fusogenic VSV mutant extended survival of mice harboring hepatocellular carcinoma xenografts compared to mice treated with the nonfusogenic VSV. They also cite experiments which indicate that these infected syncytia are more inflammatory and will result in a stronger immune response that is likely to aid in tumor clearance (32). Further, it may be possible to modulate how infected cells die in order to increase the immune response directed against tumor tissue. For example, when mitochondrial protein HMGB1 is released by a necrotic cell as opposed to an apoptotic cell, it undergoes an oxidation that modifies HMGB1 from a tolerogenic protein to an immunostimulatory protein (8, 21, 37). Thus, complete tumor clearance by direct viral oncolysis may not be necessary if, instead, an approach that induces a cell death mechanism alerts the immune system to the presence of a tumor. With the cell death pathway described here, such an approach may improve the outcomes of oncolytic virus therapy for GBM.

Two different oncolytic VSVs have recently been considered by the NIH Recombinant DNA Advisory Committee (47, 48). This is an important step in terms of the clinical development of oncolytic VSV. Observations presented here will likely advance future development of clinically approved therapy by showing that common mechanisms of resistance to chemotherapy, such as Bcl-X_L overexpression, do not necessarily lead to resistance to therapy with oncolytic viruses. They also provide a mechanistic basis for approaches such as use of small-molecule inhibitors of Bcl-2 family members that either increase the rate of tumor clearance (46) or redirect cell death in an attempt to increase antitumor immunity (32). These strategies should be explored further as oncolytic VSV enters clinical development.

ACKNOWLEDGMENTS

This work was supported by NIH grants R01 AI052304, R01 AI032983, and T32 AI007401.

We thank Peter Antinozzi for imaging assistance and his lab for the use of his equipment, Elizabeth P. Kneller for helpful discussions, Hannah Caldas for plasmids, U87 cells, and helpful discussions, and John C. Wilkinson for the use of the Bcl-X_L plasmid and helpful discussions.

REFERENCES

1. **Ahmed, M., S. D. Cramer, and D. S. Lyles.** 2004. Sensitivity of prostate tumors to wild type and M protein mutant vesicular stomatitis viruses. Virology **330:**34–49.
2. **Ahmed, M., et al.** 2003. Ability of the matrix protein of vesicular stomatitis virus to suppress beta interferon gene expression is genetically correlated with the inhibition of host RNA and protein synthesis. J. Virol. **77:**4646–4657.
3. **Ahmed, M., S. Puckett, and D. S. Lyles.** 2010. Susceptibility of breast cancer cells to an oncolytic matrix (M) protein mutant of vesicular stomatitis virus. Cancer Gene Ther. **17:**883–892.
4. **Balachandran, S., and G. N. Barber.** 2000. Vesicular stomatitis virus (VSV) therapy of tumors. IUBMB Life **50:**135–138.
5. **Balachandran, S., M. Porosnicu, and G. N. Barber.** 2001. Oncolytic activity of vesicular stomatitis virus is effective against tumors exhibiting aberrant p53, Ras, or myc function and involves the induction of apoptosis. J. Virol. **75:**3474–3479.
6. **Balachandran, S., et al.** 2000. Alpha/beta interferons potentiate virus-induced apoptosis through activation of the FADD/caspase-8 death signaling pathway. J. Virol. **74:**1513–1523.
7. **Bell, J. C., K. A. Garson, B. D. Lichty, and D. F. Stojdl.** 2002. Oncolytic viruses: programmable tumour hunters. Curr. Gene Ther. **2:**243–254.
8. **Bianchi, M. E., and A. A. Manfredi.** 2007. High-mobility group box 1 (HMGB1) protein at the crossroads between innate and adaptive immunity. Immunol. Rev. **220:**35–46.
9. **Black, B. L., and D. S. Lyles.** 1992. Vesicular stomatitis-virus matrix protein inhibits host cell-directed transcription of target genes in vivo. J. Virol. **66:**4058–4064.
10. **Black, B. L., R. B. Rhodes, M. McKenzie, and D. S. Lyles.** 1993. The role of vesicular stomatitis-virus matrix protein in inhibition of host-directed gene-expression is genetically separable from its function in virus assembly. J. Virol. **67:**4814–4821.
11. **Cattaneo, R., T. Miest, E. V. Shashkova, and M. A. Barry.** 2008. Reprogrammed viruses as cancer therapeutics: targeted, armed and shielded. Nat. Rev. Microbiol. **6:**529–540.
12. **Ebert, O., et al.** 2004. Syncytia induction enhances the oncolytic potential of vesicular stomatitis virus in virotherapy for cancer. Cancer Res. **64:**3265–3270.
13. **Ferran, M. C., and J. M. LucasLenard.** 1997. The vesicular stomatitis virus matrix protein inhibits transcription from the human beta interferon promoter. J. Virol. **71:**371–377.
14. **Freeman, A. I., et al.** 2006. Phase I/II trial of intravenous NDV-HUJ oncolytic virus in recurrent glioblastoma multiforme. Mol. Ther. **13:**221–228.
15. **Furnari, F. B., et al.** 2007. Malignant astrocytic glioma: genetics, biology, and paths to treatment. Genes Dev. **21:**2683–2710.
16. **Gaddy, D. F., and D. S. Lyles.** 2007. Oncolytic vesicular stomatitis virus induces apoptosis via signaling through PKR, Fas, and Daxx. J. Virol. **81:**2792–2804.
17. **Gaddy, D. F., and D. S. Lyles.** 2005. Vesicular stomatitis viruses expressing wild-type or mutant M proteins activate apoptosis through distinct pathways. J. Virol. **79:**4170–4179.
18. **He, S., et al.** 2009. Receptor interacting protein kinase-3 determines cellular necrotic response to TNF-alpha. Cell **137:**1100–1111.

19. **Hoffmann, D., and O. Wildner.** 2007. Comparison of herpes simplex virus- and conditionally replicative adenovirus-based vectors for glioblastoma treatment. Cancer Gene Ther. **14:**627–639.
20. **Jost, P. J., et al.** 2009. XIAP discriminates between type I and type II FAS-induced apoptosis. Nature **460:**1035–1039.
21. **Kazama, H., et al.** 2008. Induction of immunological tolerance by apoptotic cells requires caspase-dependent oxidation of high-mobility group box-1 protein. Immunity **29:**21–32.
22. **Kopecky, S. A., and D. S. Lyles.** 2003. The cell-rounding activity of the vesicular stomatitis virus matrix protein is due to the induction of cell death. J. Virol. **77:**5524–5528.
23. **Kopecky, S. A., and D. S. Lyles.** 2003. Contrasting effects of matrix protein on apoptosis in HeLa and BHK cells infected with vesicular stomatitis virus are due to inhibition of host gene expression. J. Virol. **77:**4658–4669.
24. **Kopecky, S. A., M. C. Willingham, and D. S. Lyles.** 2001. Matrix protein and another viral component contribute to induction of apoptosis in cells infected with vesicular stomatitis virus. J. Virol. **75:**12169–12181.
25. **Krakstad, C., and M. Chekenya.** 2010. Survival signalling and apoptosis resistance in glioblastomas: opportunities for targeted therapeutics. Mol. Cancer **9:**135.
26. **Kroemer, G., et al.** 2009. Classification of cell death: recommendations of the Nomenclature Committee on Cell Death 2009. Cell Death Differ. **16:**3–11.
27. **Lee, H. K., and A. Iwasaki.** 2008. Autophagy and antiviral immunity. Curr. Opin. Immunol. **20:**23–29.
28. **Lee, H. K., J. M. Lund, B. Ramanathan, N. Mizushima, and A. Iwasaki.** 2007. Autophagy-dependent viral recognition by plasmacytoid dendritic cells. Science **315:**1398–1401.
29. **Lun, X., et al.** 2006. Effects of intravenously administered recombinant vesicular stomatitis virus ($VSV^{\Delta M51}$) on multifocal and invasive gliomas. J. Natl. Cancer Inst. **98:**1546–1557.
30. **Lun, X. Q., et al.** 2009. Efficacy of systemically administered oncolytic vaccinia virotherapy for malignant gliomas is enhanced by combination therapy with rapamycin or cyclophosphamide. Clin. Cancer Res. **15:**2777–2788.
31. **Markert, J. M., et al.** 2009. Phase Ib trial of mutant herpes simplex virus G207 inoculated pre- and post-tumor resection for recurrent GBM. Mol. Ther. **17:**199–207.
32. **Melcher, A., et al.** 1998. Tumor immunogenicity is determined by the mechanism of cell death via induction of heat shock protein expression. Nat. Med. **4:**581–587.
33. **Myers, R., et al.** 2008. Toxicology study of repeat intracerebral administration of a measles virus derivative producing carcinoembryonic antigen in rhesus macaques in support of a phase I/II clinical trial for patients with recurrent gliomas. Hum. Gene Ther. **19:**690–698.
34. **Ozduman, K., G. Wollmann, S. A. Ahmadi, and A. N. van den Pol.** 2009. Peripheral immunization blocks lethal actions of vesicular stomatitis virus within the brain. J. Virol. **83:**11540–11549.
35. **Pearce, A. F., and D. S. Lyles.** 2009. Vesicular stomatitis virus induces apoptosis primarily through Bak rather than Bax by inactivating Mcl-1 and Bcl-XL. J. Virol. **83:**9102–9112.
36. **Rieger, J., U. Naumann, T. Glaser, A. Ashkenazi, and M. Weller.** 1998. APO2 ligand: a novel lethal weapon against malignant glioma? FEBS Lett. **427:**124–128.
37. **Rovere-Querini, P., et al.** 2004. HMGB1 is an endogenous immune adjuvant released by necrotic cells. EMBO Rep. **5:**825–830.
38. **Scaffidi, C., et al.** 1998. Two CD95 (APO-1/Fas) signaling pathways. EMBO J. **17:**1675–1687.
39. **Scaffidi, C., et al.** 1999. Differential modulation of apoptosis sensitivity in CD95 type I and type II cells. J. Biol. Chem. **274:**22532–22538.
40. **Shah, A. C., et al.** 2007. Enhanced antiglioma activity of chimeric HCMV/HSV-1 oncolytic viruses. Gene Ther. **14:**1045–1054.
41. **Sharif-Askari, E., et al.** 2007. Bax-dependent mitochondrial membrane permeabilization enhances IRF3-mediated innate immune response during VSV infection. Virology **365:**20–33.
42. **Stojdl, D. F., et al.** 2000. Exploiting tumor-specific defects in the interferon pathway with a previously unknown oncolytic virus. Nat. Med. **6:**821–825.
43. **Stojdl, D. F., et al.** 2003. VSV strains with defects in their ability to shutdown innate immunity are potent systemic anti-cancer agents. Cancer Cell **4:**263–275.
44. **Strik, H., et al.** 1999. BCL-2 family protein expression in initial and recurrent glioblastomas: modulation by radiochemotherapy. J. Neurol. Neurosurg. Psychiatr. **67:**763–768.
45. **Studebaker, A. W., et al.** 2010. Treatment of medulloblastoma with a modified measles virus. Neuro. Oncol. **12:**1034–1042.
46. **Tumilasci, V. F., et al.** 2008. Targeting the apoptotic pathway with BCL-2 inhibitors sensitizes primary chronic lymphocytic leukemia cells to vesicular stomatitis virus-induced oncolysis. J. Virol. **82:**8487–8499.
47. **U. S. Department of Health and Human Services.** 2008. Minutes of the Recombinant DNA Advisory Committee 12/3–4/2008. Recombinant DNA Advisory Committee, U. S. Department of Health and Human Services, Rockville, MD. http://oba.od.nih.gov/oba/RAC/meetings/dec2008/RAC_Minutes_12-08.pdf.
48. **U. S. Department of Health and Human Services.** 2008. Minutes of the Recombinant DNA Advisory Committee 9/9–10/08. Recombinant DNA Advisory Committee, U. S. Department of Health and Human Services, Rockville, MD. http://oba.od.nih.gov/oba/RAC/meetings/Sept2008/RAC_Minutes_09-08.pdf.
49. **Wilkinson, J. C., E. Cepero, L. H. Boise, and C. S. Duckett.** 2004. Upstream regulatory role for XIAP in receptor-mediated apoptosis. Mol. Cell. Biol. **24:**7003–7014.
50. **Wilkinson, J. C., et al.** 2004. VIAF, a conserved inhibitor of apoptosis (IAP)-interacting factor that modulates caspase activation. J. Biol. Chem. **279:**51091–51099.
51. **Wollmann, G., M. D. Robek, and A. N. van den Pol.** 2007. Variable deficiencies in the interferon response enhance susceptibility to vesicular stomatitis virus oncolytic actions in glioblastoma cells but not in normal human glial cells. J. Virol. **81:**1479–1491.
52. **Wollmann, G., V. Rogulin, I. Simon, J. K. Rose, and A. N. van den Pol.** 2010. Some attenuated variants of vesicular stomatitis virus show enhanced oncolytic activity against human glioblastoma cells relative to normal brain cells. J. Virol. **84:**1563–1573.
53. **Wollmann, G., P. Tattersall, and A. N. van den Pol.** 2005. Targeting human glioblastoma cells: comparison of nine viruses with oncolytic potential. J. Virol. **79:**6005–6022.
54. **Yin, X. M.** 2000. Signal transduction mediated by Bid, a pro-death Bcl-2 family proteins, connects the death receptor and mitochondria apoptosis pathways. Cell Res. **10:**161–167.
55. **Yin, X. M., et al.** 1999. Bid-deficient mice are resistant to Fas-induced hepatocellular apoptosis. Nature **400:**886–891.
56. **Zemp, F. J., J. C. Corredor, X. Lun, D. A. Muruve, and P. A. Forsyth.** 2010. Oncolytic viruses as experimental treatments for malignant gliomas: using a scourge to treat a devil. Cytokine Growth Factor Rev. **21:**103–117.